EARTH SCIENCES
RESEARCH JOURNAL

Earth Sci. Res. J. Vol. 12, No. 1 (June 2008): 7-30

A NEW INTERPRETATION FOR THE GARNET ZONING IN METAPELITIC ROCKS OF THE SILGARÁ FORMATION, SOUTHWESTERN SANTANDER MASSIF, COLOMBIA

Carlos Alberto Ríos Reyes[1], Oscar Mauricio Castellanos Alarcón[2] and Akira Takasu[3]

[1] *Escuela de Geología, Universidad Industrial de Santander, A.A 678, Bucaramanga, Colombia.*
[2] *Programa de Geología, Universidad de Pamplona, Colombia.*
[3] *Geosciences Department, Shimane University, Japan.*

Corresponding author: Carlos Alberto Ríos Reyes, School of Applied Sciences, University of Wolverhampton, Wulfruma Street, Wolverhampton WV1 1SB, UK
Tel. +44 (0)1902 322679; Fax. +44 (0)1902 322714; E-mail: C.A.RiosReyes@wlv.ac.uk

Abstract

A Barrovian sequence of the Silgará Formation at the southwestern Santander Massif, Colombian Andes, contains zoned garnets in which major and trace element zoning correlates with distribution of mineral inclusions, which may indicate that garnet growth rate varied through time and affected both composition and texture of garnets, although different garnet producing reactions have also played an important role in the chemical zoning of garent. However, a local metasomatism process associated to the action of late magmatic fluids associated to the emplacement of the Pescadero Pluton (external forcing mechanism) would be also considered. In particular, Ca, Mn and Y zoning patterns in some garnets correspond with inclusion-rich vs. inclusion-free zones, although the distribution of inclusions does not correlate with chemical zoning (i.e., the same inclusions are found in Ca-rich and Ca-poor zones of the garnet). There is a similar lack of correlation with accessory phases (apatite, monazite, xenotime, ilmenite or rutile). In a garnet from the garnet-staurolite zone, a high Mn core contains abundant and randomly oriented apatite, monazite and ilmenite inclusions, while a euhedral low Ca mantle zone is inclusion-free and the high Ca / low Mn rim zone contains apatite, monazite and ilmenite aligned parallel to the margins of the garnet. Inclusions in garnet can also represent mineral phases were not completely consumed during garnet growth. Association of garnet zoning trends and patterns with inclusion distribution may help differentiate between processes that identically affect major-element zoning but that produced variable textures in the garnet.

Manuscript received September 7, 2007.
Accepted for publication January 30, 2008.

Key words: Colombia; garnet; zoning; Santander Massif; Silgará Formation.

Resumen

Una secuencia Barroviana de la Formación de Silgará en la región suroccidental del Macizo de Santander, Andes colombianos, contiene granates zonados en los cuales la zonación de elementos mayores y trazas se correlaciona con la distribución de las inclusiones minerales, lo cual puede indicar que la tasa de crecimiento del granate varió con el tiempo y afectó la composición y la textura de los granates, aunque diferentes reacciones que producen granate han jugado también un papel importante en la zonación química del granate. Sin embargo, un proceso local de metasomatismo generado por la acción tardia de fluidos magmáticos asociados al emplazamiento del Plutón de Pescadero (mecanismo de fuerza externa) es también aquí considerado. En particular, los patrones de zonación de Ca, Mn e Y en algunos granates corresponden con zonas ricas en inclusiones vs. zonas sin inclusiones, aunque la distribución de inclusiones no se correlaciona con la zonación química (es decir, las mismas inclusiones se encuentran en las zonas ricas y pobres en Ca del granate). Hay una carencia similar de correlación con las fases accesorias (apatito, monacita, xenotima, ilmenita o rutilo). En un granate de la zona del granate-estaurolita, un núcleo alto en Mn contiene abundantes inclusiones aleatoriamente orientadas de apatito, monacita e ilmenita, mientras que una zona euhedral baja en Ca carece de inclusiones y la zona de borde rica de alto Ca / bajo Mn contiene inclusiones de apatito, monacita, e ilmenita orientadas paralelo a los bordes del granate. Inclusiones en granate pueden también representar fases minerales que no fueron completamente consumidas durante el crecimiento del granate. La asociación de los patrones de zonación del granate con la distribución de las inclusiones puede ayudar a distinguir entre los procesos que afectan idénticamente la zonación de elementos mayores pero produjo texturas variables en el granate.

Palabras claves: Colombia; granate; zonación; Macizo de Santander; Formación Silgará.

Introduction

Garnet is one of the most studied minerals in relation with chemical variations in metamorphic rocks since it preserves a record of its growth history expressed by the chemical zoning and inclusions of other minerals. The broad range in mineral composition promotes the growth of garnet in rocks of very different chemical compositions and over a wide spectrum of metamorphic conditions. Furthermore, its refractory character allows the preservation of chemical and textural zoning that is important when making interpretations about the metamorphic history of the host rock. Of particular interest in recent years have been the trace element zoning in garnet as an important source of information for petrologic processes (Hickmott & Shimizu, 1990; Schwandt *et al.,* 1996; Chernoff & Carlson, 1999; Yang & Rivers, 2001; Skelton *et al.,* 2002) and for relating the growth of geochronologically important accessory phases (e.g., monazite) to metamorphic reaction histories (Pyle & Spear, 1999; Gibson *et al.*, 2004). Major and trace element zoning in garnet have been typically explained by (1) elemental fractionation during mineral growth (e.g., Hollister 1966; Cygan and Lasaga 1982), (2) by intracrystalline diffusion (e.g., Anderson and Buckley 1973), (3) limitations at the mineral-matrix interface (e.g., Carlson 1989), (4) interaction with a metasomatic fluid (e.g., Hickmott *et al.* 1987; Young and Rumble 1993; Chamberlain and Conrad 1993; Erambert and Austrheim 1993; Jamtveit *et al.* 1993; Jamtveit and Hervig 1994), (5) the breakdown or growth of trace element-rich minerals (Hickmott & Shimizu, 1990; Hickmott and Spear 1992) or (6) changes in the garnet-mineral matrix partition coefficients because of changes in pressure and temperature conditions, garnet composition or the number of mineral phases in the assemblage or their proportions

(Yang and Rivers, 2002). The majority of these processes occur during crystal growth. Diffusional reequilibration is the only primary postgrowth process that leads to zoning in minerals. In an extreme case, compositional zoning can arise in garnet after its crystallization with a homogeneous composition that is in desequilibrium with the matrix. Because a chemical gradient exists between the garnet and the surrounding matrix, often biotite-rich, volume diffusion acts to reequilibrate the garnet composition with the matrix (e.g., Tracy *et al.*, 1976). Diffusion occurs as long as the temperature remains sufficiently high (e.g., Lasaga 1983). Trace elements are extremely sensitive to changes in accessory mineral assemblage and/or fluid composition and many trace-element diffusivities in garnet must be very much slower than diffusivities for major elements (Mg, Mn, Fe) in garnet, but probably on the same order as the diffusivity of Ca in garnet (Pyle & Spear, 1999). Trace element distributions in garnet must, however, be interpreted with caution. Previous studies have documented trends in Ca, Mn and Y zoning in garnet (e.g., Chernoff & Carlson, 1997; Pyle & Spear, 1999; Yang & Rivers, 2002) and discussed the possibility that low- or high- annuli within garnet are related to local disequilibrium in some elements, but not all. For example, patterns that deviate from normal growth zoning in garnet (e.g., euhedral bands concentric about the garnet core, patches or spiral to curving patterns) might form by garnet overgrowth of phases enriched or depleted in particular major or trace elements (e.g., Mn; Yang & Rivers, 2001; Hirsch *et al.*, 2003), by resorption of garnet during garnet-consuming reactions that produce staurolite (Menard & Spear, 1993) or by growth of garnet after a matrix phase has been depleted (e.g., epidote, chloritoid; Whitney & Ghent, 1993). The resulting garnet zoning patterns will be a function of the local chemical heterogeneities, the temperature of metamorphism during and after garnet growth and the growth rate of garnet, factors that will affect both the zoning and the distribution of mineral inclusions in garnet. Chernoff & Carlson (1997, 1999) considered the possibility of independent, local scales of equilibrium for different elements. They demonstrated that many trace elements, as well as Ca, reflect disequilibrium at thin-section scale and therefore thermobarometric estimates that involve grossular contents may be in error. Garnet zoning may also be affected by fluid flow (e.g., Stowell *et al.* 1996; Skelton *et al*., 2002) and deformation and these processes may be coupled, as deformation will change grain size and adjust grain boundaries, affecting rates and pathways for diffusion. Garnets are frequently zoned in the major elements Fe, Mg, Mn and Ca. At high temperature, major element growth zoning may be significantly modified by intracrystalline diffusion while trace element zoning may be less susceptible to diffusion (e.g., Hickmott & Spear, 1992; Lanzirotti, 1995; Chernoff & Carlson, 1999). In this paper, we report zoning patterns for garnets of the metapelitic Silgará Formation of the southwestern Santander Massif, Colombian Andes. We document major and trace element zoning in garnets and evaluate the processes that control and influence zoning during prograde metamorphism.

Geological setting

The Santander Massif lies within the Eastern Cordillera of the Colombian Andes, where it divides into the northeast-trending Perijá in Colombia and the east-northeast-trending Mérida Andes in Venezuela (Figure 1). The metamorphic history of this massif is important for interpretation of the geologic and tectonic evolution of the northwestern continental margin of South America. The Santander Massif is underlain by deformed and metamorphosed rocks that have been tectonostratigraphically divided into three metamorphic units (Bucaramanga Gneiss Complex, Silgará Formation and Orthogneiss), which are intruded by several igneous bodies, most of them of Triassic-Jurassic age and some of Paleozoic age (e.g., Goldsmith *et al*., 1971; Boinet *et al.*, 1985; Dörr *et al.*, 1995; Ordoñez, 2003). The intrusives form part of the Santander Plutonic Complex and are interpreted as calc-alkaline crustal bodies emplaced after peak-metamorphism. Sedimentary rocks ranging in age from Devonian to Tertiary flank the core rocks. The garnet-bearing samples investigated in the present study belong to the metapelitic sequence of the Caledonian Silgará Formation that represents what was originally a very thick pile of volcano-sedimentary rocks. Well-exposed sections of this metamorphic unit crop out at the southwestern region of the Santander Massif (Figure 1), which is long established as classic area for the study of rock metamorphism and deformation caused by continental collision during the Caledonian orogeny. According to Ríos et al. (2003), this region experienced crustal thickenning during the initial stages of collision, followed by a slow uplift and erosion period, resulting in a decompression accompanied by heating. The Silgará Formation structures and metamorphic features here are complex and early workers had great difficulty in making sense of the geology of the area. The metamorphic rocks of the Silgará Formation generally strike NW-SE and dip to the southwest. The NW-trending Bucaramanga Fault represents a very major break in the crust in the northeastern part of the

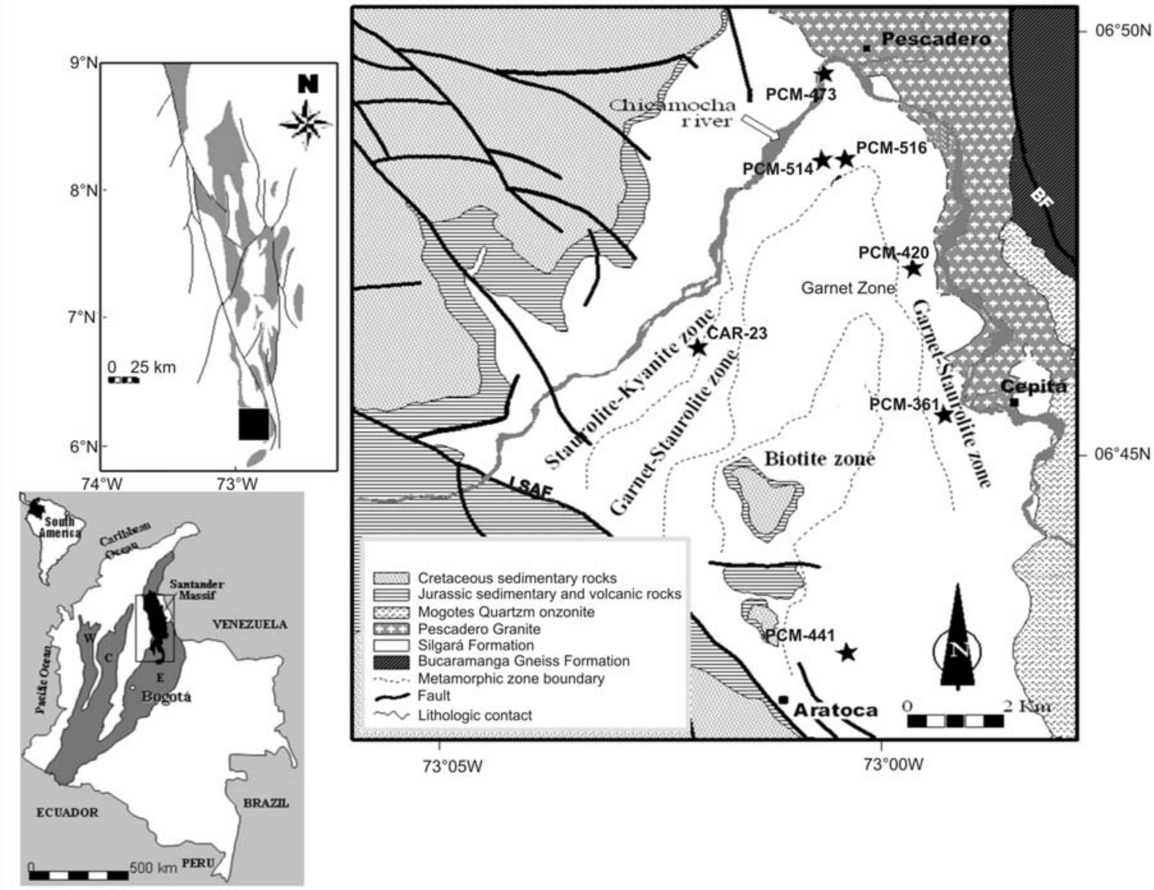

Figure 1. Lower left side, map of the Colombian Andes, showing the location of the Santander Massif in the Eastern Cordillera. Upper left side, simplified geological map of the Santander Massif, showing the distribution of the Silgará Formation metamorphic rocks in grey (modified after Goldsmith *et al.*, 1971) and the location of the study area in black. Right side, generalized geological map of the study area (modified after Ward *et al.*, 1973), showing locations of garnet samples investigated (black stars). Metamorphic zones modified after Ríos *et al.* (2003). BF: Bucaramanga Fault; LSAF. Los Santos - Aratoca Fault.

study area and separates the Precambrian Bucaramanga Gneiss Complex from the Triassic-Jurassic Pescadero and Mogotes batholiths. This fault is probably strike slip with a protracted history of displacement (Goldsmith *et al.*, 1971). In the southwest, near Aratoca, the Silgará Formation is cut by the NW-SE-trending Los Santos - Aratoca Fault and is unconformably overlain by Mesozoic sedimentary rocks (Figure 1). It is also unconformably overlain by a Mesozoic sequence on the northwest and the southwest. The Triassic-Jurassic Pescadero and Mogotes batholiths intruded the Silgará Formation in the northeastern and eastern part of the area after peak-metamorphism (Goldsmith *et al.*, 1971). The Silgará Formation is dominated by metapelitic rocks with minor intercalations of metabasites. The lithology of the metapelitic sequence changes in composition northeastward, from quartz-rich pelitic schists in the southwest to feldspar-rich semipelitic schists in the northeast. A millimeter-scale compositional banding consists of alternating granoblastic quartz-plagioclase-rich domains with minor K-feldspar and muscovite-biotite-rich domains. Subordinated rock types of the Silgará Formation are well-foliated amphibole-bearing schists, orthoamphibolites and calc-silicate rocks. Microstructural evidence shows that the Silgará Formation underwent prograde metamorphism during at least three deformation phases, including extensive retrograde metamorphism during the last stage. The dominant schistosity or slaty cleavage in the metapelitic rocks may have developed at the same time as early folds and thrusts. The metapelites display a well-developed schistosity, although well-preserved sedimentary features are locally preserved in low-grade rocks. In general, later structures such as flat-lying crenulations, small chevron folds and kink bands overprint the main foliation. Retrograde textures include partial replacement of garnet by chlorite and/or muscovite or chlorite and biotite along cracks; heavily corroded staurolite crystals surrounded by muscovite; biotite and calcic-amphibole replaced by chlorite (although in some cases amphibole is replaced by biotite); and feldspar partly replaced by sericite. A progressive sequence of metamorphic zones has developed in pelitic rocks of the Silgará Formation. The regional metamorphic grade increases with structural depth from the biotite zone to the staurolite-kyanite zone. Garnet-bearing pelites are widespread throughout the region. Barrovian regional metamorphism occurred under low- to high-temperature and medium-pressure conditions. The distinction between the staurolite-kyanite and lower sillimanite (fibrolite) zones is not well defined because fibrolitic sillimanite is present in trace amounts in staurolite-kyanite bearing samples. The occurrence of fibrolite in sample PCM-473 lacking other Al_2SiO_5 phases near the contact with the Pescadero Pluton is interpreted as formed in the waning stages of a thermal event. Therefore, the fibrolitization process should not be always considered as a polymorphic reaction. Ríos *et al.* (2003) estimated the temperatures and pressures of equilibration of mineral assemblages from metamorphic rocks of the southwestern Santander Massif. P-T conditions were 500-520°C and 4.4-5.5 kbar in the garnet zone and 590-700°C and 5.5-7.5 kbar in the garnet-staurolite zone.

Analytical methods

X-ray maps were collected and analyses were carried out using the JEOL 8800 electron probe microanalyzer at the Research Center for Coastal Lagoon Environments at the Shimane University (Japan) and the JEOL 8900 electron probe microanalyzer at the Department of Geology and Geophysics at the University of Minnesota (USA). Accessory mineral phases were identified using back-scattered electron imaging (BEI) and energy-dispersive spectroscopy (EDS). The analytical conditions were as follows: accelerating voltage of 15 kV and beam current of 20-25 nA (for quantitative analyses) and 25-75 nA (with dwell times of 40-55 msec/pixel, for major element maps) or higher beam current (100 nA) and longer dwell times (up to 90 msec/pixel) for trace element maps. Qualitative X-ray maps were obtained first to delineate geochemically significant zones and to guide quantitative spot analysis (in radial traverses and spacing decreasing near the rim). Data adquisition and reduction were carried out using the ZAF correction procedures. A combination of natural and synthetic minerals were used as standards.

Chemical zoning and textural relations in garnet

A detailed petrographic study of six thin sections was carried out on selected specimens which are the same as those studied by Ríos (1999) and corresponding to a series of pelitic rocks of the Silgará Formation composed of quartz + plagioclase + muscovite + biotite + garnet ± staurolite and accessory fibrolitic sillimanite and rare crystals of andalusite and kyanite (one sample contained the three polymorphs). In the garnet zone, garnets are commonly idioblastic, whereas in the garnet-staurolite and staurolite-kyanite zones they tend to be rounded and embayed, displaying reaction rims. As follows we describe petrographic features of the major and accessory minerals in the analyzed samples as illustrated in Figure 2. The mineral assemblages of the analyzed samples are given in Table 1. Mineral abbreviations are after Kretz (1983). All the examined samples contain garnet porphyroblasts that preserve growth zoning to varying degrees. Garnet is almandine-rich and exhibits zoning in which Mn decreases from core to rim as Mg and Fe increase. The zoning of Fe, Mg and Mn zoning is strongly correlated with respect to the degree of local equilibrium in contrast with Ca zoning that does not mimic Fe, Mg and Mn zoning exactly (e.g., Chernoff & Carlson, 1997; Spear & Daniel, 1998). According to Hirsch *et al.* (2003), it reflects a combination of changing availability of these elements to the surface of the growing garnet and changing partitioning of elements among the mineral phases in the rock. Garnet shows abrupt variations in Ca distribution from core to rim, developing in some cases a complex cyclic zoning with euhedral low- or high-Ca annuli. Trace element zoning in garnet will depend on the presence or absence of saturing phases, such as xenotime for Y, xenotime, apatite or monazite for P and ilmenite, titatine and rutile for Ti. Analyzed garnets do not show zoning in Y, Sc, P, Cr or Ti, except garnet zone sample PCM-441, which exhibits Y zoning. Yttrium is potentially useful for monitoring reactions involving Ca-rich minerals such as epidote and plagioclase because this element substitutes for Ca in mineral structures and Y discontinuities in garnet zoning may correlate with inflections in Ca zoning (Hickmott & Spear, 1992). In the following sections, we describe the main features of chemical zoning in garnet from the Silgará Formation pelites. Table 2 shows representative chemical compositions of analyzed garnets. Analytical points are indicated by white dots and numbers in the X-ray maps, with numbers keyed to the table.

PCM-441 Garnet. Pelitic schist from the garnet-zone, which typically contain a mineral assemblage of muscovite + quartz + plagioclase + garnet ± biotite, with minor K-feldspar, tourmaline, apatite, zircon, epidote, calcite and Fe-Ti oxides. Numerous, very fine-grained (0.03-0.42 mm in diameter), euhedral grains of garnet, with a hexagonal or pentagonal outline, occur in this sample (Figure 2a). Garnet grew after an early foliation and contain inclusion trails of ilmenite and graphite concordant to the main foliation (crenulation cleavage), although it may have inclusion-free rims. It is replaced along their margins and fractures by chlorite, biotite and Fe-oxides. The most striking characteristic of this garnet is the high Mn concentration, which from core to rim varies from 54 to 25 mol% spessartine (Figure 3a). Fe and Mg increase from core to rim with a small decrease in Fe/Fe+Mg. Garnet has a low-Ca core (7 mol%) with an inflection midway (14 mol%) between core and rim, decreasing towards the rim (8 mol%), as shown in Figure 4a. Trace element maps for garnet in sample PCM-441 show that yttrium is the only one that displays zoning. With the possible exception of Yb, which shows a slight enrichment in the garnet core, the other trace elements (Sc, P, Cr, Ti and Yb) are in low abundance and homogeneous across the garnet. Garnet is characterized by a euhedral outline, high-Y core (Figure 4b), which is larger than the faint Yb-rich region. The Y-rich core region corresponds exactly to the low Ca core region. Relatively Y-enriched regions of the garnet also occur discontinuously along the rim and in the Ca-poor core of

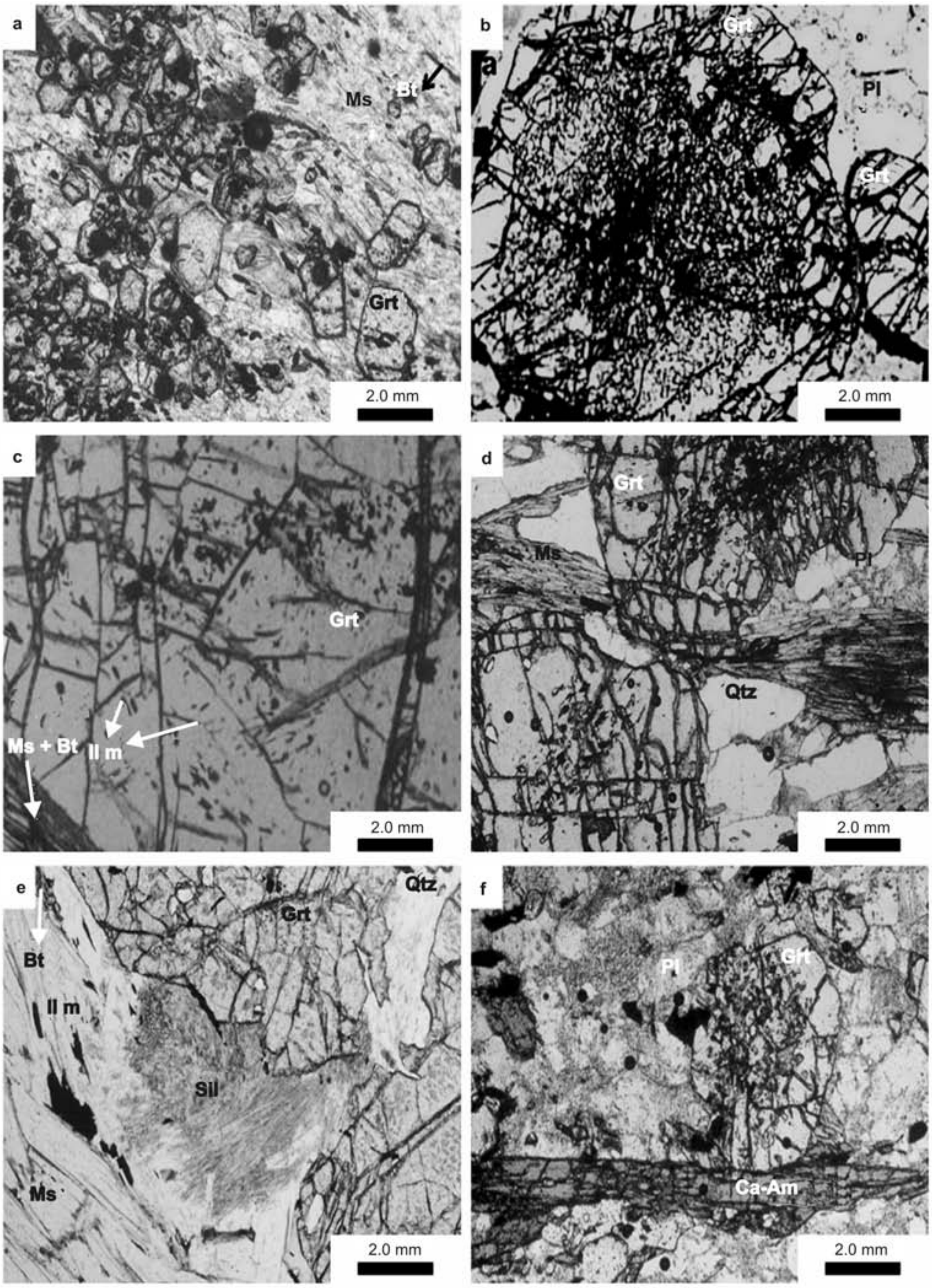

Figure 2. Plane-polarized light photomicrographs of garnet-bearing metamorphic rocks of the Silgará Formation. (a) Numerous very fine-grained garnet crystals; sample PCM-441 (garnet zone). (b) Garnet with inclusion-rich (quartz and ilmenite) core and inclusion-free rim regions; sample PCM-420 (garnet-staurolite zone). (c) Garnet porphyroblast displaying two different inclusion patterns involving ilmenite; sample PCM-361 (garnet-staurolite zone). (d) Inclusion trails of quartz and ilmenite preserved in garnet porphyroblasts; sample PCM-516 (garnet-staurolite zone). (e) Fibrolitic sillimanite occurring at core of muscovite adjacent to garnet; sample PCM-473 (staurolite-kyanite zone). (f) Garnet-bearing calc-silicate rock occurring as numerous fine- to medium-grained crystals associated with calcic amphibole; sample PCM-514 (garnet-staurolite zone).

Table 1. Mineral assemblages of the analyzed samples of the Silgará Formation pelitic rocks from the southwestern Santander Massif

Met. Zone	Sample	Chl	Bt	Ms	Qz	Pl	Kfs	Grt	St	And	Ky	Sil	Ca-A	Zr	Ap	Mgn	Ilm	Rut	Ep	Mnz	Xen	Tur	Cal
Garnet	PCM-441	r	X	X	X	X	m	X						m	m		m		m			m	r
Garnet-St aurolite	PCM-361	r	X	X,r	X,i	X		X	X					i	i		i	i		i	i		
Garnet-St aurolite	PCM-516	r	X	X	X,i	X	X	X							I		I						
Garnet-St aurolite	PCM-514	r	X,i		X,i	X,i	X,i	X					X,i		i	i	i		i				r
Garnet-St aurolite	PCM-420	r	X		X,i	X,i	X	X								i	i						
Staurolite-Kyanite	PcM-473	r	X,i	X,r,i	X,i	X,i		X	X			m,i				i		m				m	

Qtz, Bt, Pl, and retrograde Chl are common in all samples. X-present, blank-absent, m-minor phase, i-inclusions in garnet, r-retrograde minerals.
Mineral abbreviations after Kretz (1983)

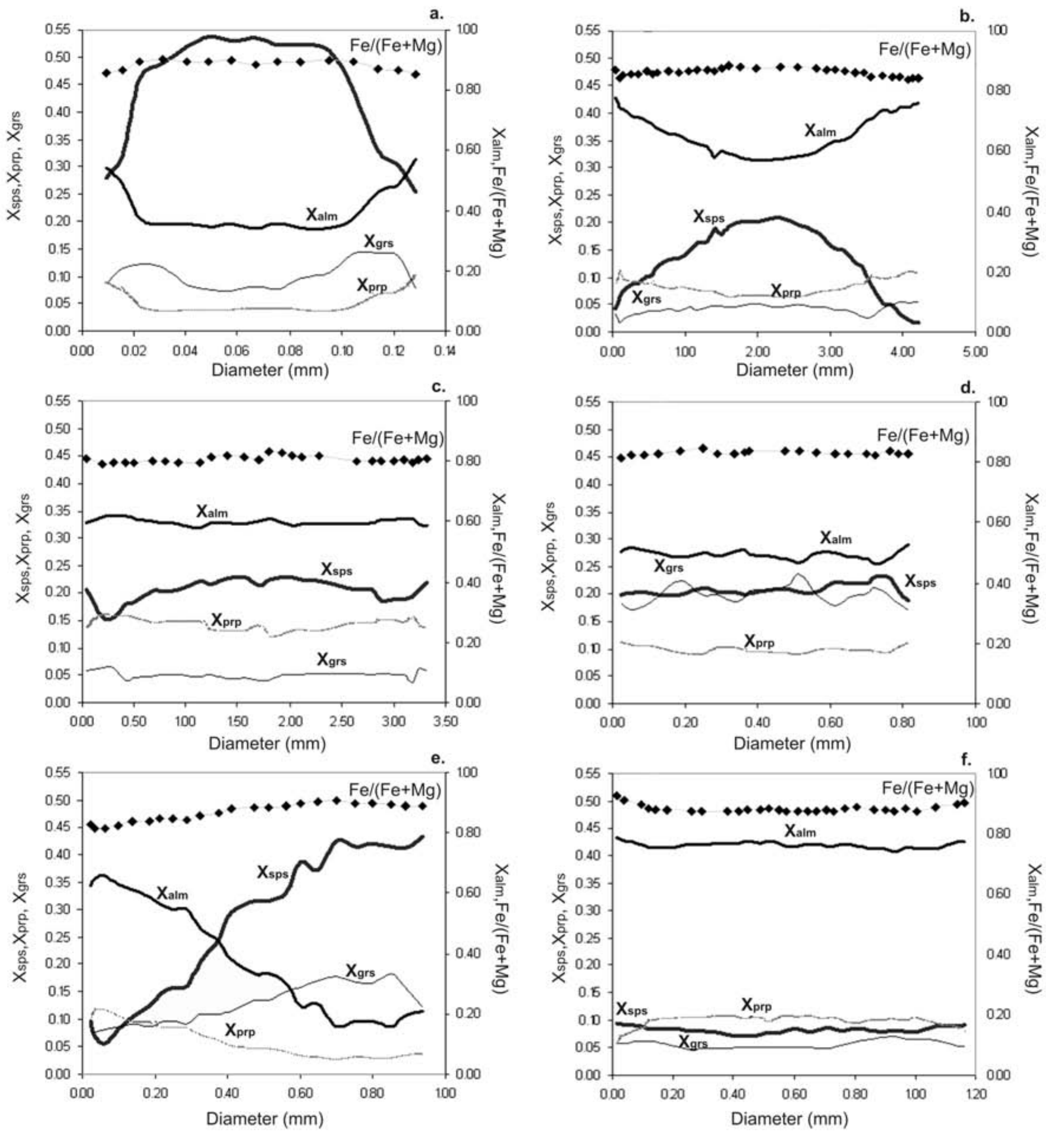

Figure 3. Zoning profiles rim-core-rim of almandine, pyrope, spessartine and grossular components and Fe/(Fe+Mg) ratio in garnet from samples (a) PCM-441 (garnet zone), (b) PCM-514 (garnet-staurolite zone), (c) PCM-361 (garnet-staurolite zone), (d) PCM-516 (garnet-staurolite zone), (e) PCM-420 (garnet-staurolite zone) and (b) PCM-473 (staurolite-kyanite zone). Note the different scales for X_{sps}, X_{prp} and X_{grs} on the left and for X_{alm} and Fe/(Fe+Mg) on the right.

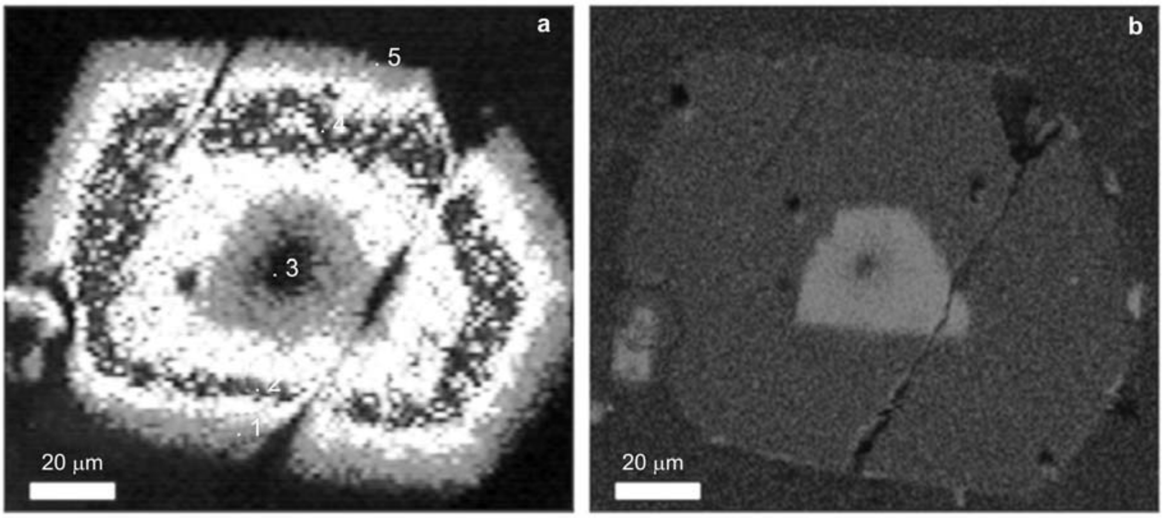

Figure 4. X-ray compositional maps in garnet from sample PCM-441 (garnet zone). (a) Ca map, showing a high-Ca band at mantle region and the relationship between the low-Ca at core and the high-Y annulus. Numbered spots are keyed to analyses in Table 2. (b) Y map, displaying a high-Y annulus at core characterized by sharp euhedral and straight outlines. In the X-ray maps, the elemental distributions are indicated by white color for the highest and black color for the lowest concentration.

an adjacent small garnet. X-ray maps for Ca distribution in garnet and its vicinity indicate that there are no Ca-rich accessory phases included in garnet and only one small apatite crystal in the matrix just beyond the field of view in Figure 4.

PCM-361 Garnet. Pelitic schist from the garnet-staurolite-zone characterized by the peak metamorphic assemblage of quartz + plagioclase + muscovite + biotite + garnet + staurolite. Garnet porphyroblasts (1.5-2.6 mm in diameter) are anhedral to subhedral with an elliptical outline and contain numerous inclusions of ilmenite that define different pattern of distribution (Figure 2c). At the core region, the inclusion patterns can be concordant or discordant to the main foliation of the rock or ramdonly oriented, whereas at the rim region, they follow the rim of the garnet, defining an approximately circular pattern. Garnet porphyroblasts area wrapped by a penetrative foliation (crenulation cleavege). Garnet is strongly zoned in Mn (Figures 3c, 5b), which decreases from 21 mol% in the core to 1-2 mol% in the rim. Fe and Mg increase from core to rim, with a small decrease in Fe/Fe+Mg. Ca decreases from core (5 mol%) towards the rim, with a slight discontinuity in the zoning midway between core and rim, reaching a minimum (1-2 mol%) represented by an euhedral low-Ca annulus (Figures 5a, 6a); then increases towards the rim (6 mol%). The low-Ca annulus coincides with the euhedral zone of high-Mn (6-9 mol%) and is truncated in the bottom part due to partial resorption of garnet. Analyzed garnets all exhibit complex Ca zoning, but there is no apparent zoning in analyzed trace elements (Y, Yb, P, Ti, Cr). Garnet is texturally zoned with respect to the distribution and shape orientation of ilmenite inclusions and textural zoning can be related to chemical zoning (Figures 2c, 5, 6a). In the Mn-rich garnet core region, ilmenite inclusions are randomly oriented. Inclusions are absent in the low-Ca annulus. In the high-Ca / low-Mn near-rim zone, ilmenite inclusions are abundant and are aligned parallel to the garnet rim, creating a circular pattern, which is also apparent in matrix ilmenite adjacent to garnet (Figure 2c). Ilmenite occurs as inclusions in garnet that have been partially pseudomorphed by rutile (Figure 7) or as a matrix accessory mineral. Other inclusions in garnet are quartz, apatite, monazite, zircon and rutile, which

Table 2. Representative compositions of metamorphic garnet from the Silgará Formation, southwestern Santander Massif.

Major elements	PCM-441					PCM-31							PCM-516	PCM-514								PCM-420				PCM-473			
	rim		core		rim	rim			core			rim	rim	rim				core			rim	core			rim	rim	core	rim	
wt%	1	2	3	4	5	1	2	3	4	5	6	7	1	1	2	3	4	5	6	7	8	1	2	3	4	1	2	3	4
SiO_2	36,39	36,76	36,17	36,96	36,82	37,73	37,45	36,76	36,79	36,67	36,69	37,10	37,61	36,88	37,31	36,62	37,44	36,76	37,33	36,85	37,66	36,63	36,5	37,26	36,76	37,38	37,45	37,30	37,67
TiO_2	0,02	0,06	0,08	0,05	0,05	0,00	0,00	0,09	0,12	0,00	0,01	0,05	0,02	0,04	0,02	0,12	0,16	0,46	0,05	0,03	0,03	0,13	0,02	0,00	0,00	0,08	0,00	0,00	0,04
Al_2O_3	20,64	20,32	20,03	20,59	20,69	20,61	20,49	20,53	20,55	20,52	20,63	20,41	19,91	20,28	20,19	20,46	19,81	19,17	20,46	20,31	20,70	19,79	20,24	20,63	20,25	20,10	20,46	20,50	20,23
FeO*	25,42	17,95	16,61	22,13	26,26	38,86	37,07	33,84	32,10	34,65	34,94	37,75	27,92	23,39	23,46	22,64	23,80	22,55	22,92	21,45	23,85	24,66	25,72	32,09	31,22	34,83	34,17	34,91	34,15
MnO	12,28	20,34	22,92	14,52	11,20	1,91	2,78	6,51	9,21	5,58	4,99	0,75	9,27	8,72	8,85	8,85	9,14	9,24	9,79	10,14	8,42	13,89	11,6	3,43	4,68	3,39	2,57	3,73	3,8
MgO	2,26	1,12	0,98	1,72	2,47	2,29	2,76	2,04	1,68	2,21	2,22	2,77	3,51	2,86	2,76	2,40	2,65	2,36	2,59	2,43	2,81	1,57	1,72	2,77	2,47	1,72	2,85	1,78	2,03
Ca O	2,95	4,22	2,52	5,02	2,76	1,21	0,63	1,60	1,61	1,27	0,97	1,93	2,09	6,39	5,98	7,91	6,56	7,52	6,25	7,31	5,98	3,52	3,60	2,97	2,72	1,88	2,16	1,85	2,00
Na_2O	0,00	0,01	0,07	0,03	0,01	0,04	0,06	0,04	0,06	0,05	0,03	0,04	0,04	0,03	0,06	0,03	0,03	0,04	0,03	0,00	0,02	0,01	0,04	0,00	0,01	0,02	0,01	0,05	0,05
K_2O	0,06	0,04	0,05	0,04	0,17	0,07	0,05	0,05	0,06	0,03	0,05	0,04	0,08	0,08	0,04	0,06	0,05	0,04	0,05	0,03	0,04	0,04	0,05	0,05	0,05	0,04	0,04	0,01	0,08
Cr_2O_3	0,00	0,00	0,00	0,00	0,00	0,04	0,01	0,00	0,03	0,00	0,00	0,07	0,00	0,01	0,00	0,00	0,01	0,02	0,00	0,02	0,00	0,01	0,00	0,01	0,02	0,00	0,01	0,02	0
Total	100,01	100,82	99,43	101,07	100,43	102,25	101,28	101,46	102,20	100,98	100,82	100,90	100,45	98,68	98,67	100,09	99,65	98,16	99,47	98,57	99,51	100,25	99,49	99,21	98,18	99,42	99,73	100,19	100,04
Cations based on 12 atoms of oxygen																													
Si	2,961	2,982	2,99	2,974	2,978	3,012	3,011	2,970	2,963	2,974	2,994	2,992	3,027	2,996	3,03	3,008	3,020	3,01	3,01	3	3,020	2,991	2,989	3,020	3,021	3,052	3,028	3,026	3,052
Ti	0,001	0,004	0,01	0,003	0,003	0,000	0,000	0,005	0,007	0,000	0,001	0,003	0,001	0,002	0	0,007	0,010	0,03	0	0	0,002	0,008	0,001	0,000	0,000	0,005	0,000	0,000	0,003
Al	1,979	1,942	1,95	1,952	1,972	1,938	1,941	1,955	1,95	1,961	1,967	1,939	1,888	1,941	1,930	1,928	1,88	1,85	1,94	1,95	1,956	1,905	1,953	1,971	1,961	1,934	1,950	1,965	1,932
Fe^{3+}	0,096	0,087	0,07	0,093	0,066	0,038	0,038	0,094	0,109	0,091	0,042	0,072	0,056	0,062	0,017	0,041	0,058	0,06	0,04	0,06	0,000	0,097	0,067	0,000	0,000	0,000	0,000	0,000	0,000
Fe^{2+}	1,633	1,13	1,08	1,396	1,710	2,522	2,454	2,193	2,053	2,259	2,322	2,474	1,823	1,526	1,57	1,473	1,55	1,482	1,510	1,4	1,599	1,587	1,694	2,175	2,146	2,378	2,310	2,368	2,314
Mn	0,846	1,397	1,6	0,090	0,767	0,129	0,189	0,445	0,628	0,383	0,342	0,051	0,632	0,600	0,608	0,599	0,62	0,64	0,67	0,7	0,572	0,961	0,804	0,235	0,326	0,234	0,176	0,256	0,261
Mg	0,275	0,135	0,12	0,206	0,298	0,273	0,331	0,246	0,202	0,267	0,268	0,333	0,421	0,346	0,33	0,286	0,32	0,29	0,31	0,29	0,336	0,191	0,210	0,335	0,303	0,209	0,344	0,215	0,246
Ca	0,257	0,367	0,22	0,432	0,239	0,103	0,054	0,138	0,139	0,110	0,084	0,167	0,180	0,556	0,520	0,678	0,57	0,660	0,540	0,64	0,514	0,308	0,316	0,258	0,239	0,164	0,187	0,161	0,173
Na	0,001	0,003	0,03	0,011	0,002	0,011	0,018	0,012	0,018	0,016	0,009	0,013	0,013	0,010	0,020	0,01	0,010	0,013	0,010	0,000	0,006	0,003	0,013	0,000	0,003	0,006	0,002	0,015	0,015
K	0,012	0,009	0,010	0,009	0,036	0,014	0,010	0,011	0,012	0,006	0,011	0,007	0,017	0,017	0,01	0,013	0,01	0,01	0,01	0,01	0,009	0,009	0,011	0,011	0,011	0,008	0,009	0,003	0,018
Cr	0,000	0,000	0,000	0,000	0,000	0,002	0,000	0,000	0,002	0,000	0,000	0,004	0,000	0,001	0,000	0,000	0	0	0,000	0	0,000	0,001	0,000	0,001	0,001	0,000	0,001	0,001	0,000
Total	8,061	8,056	8,07	8,067	8,071	8,043	8,046	8,070	8,084	8,067	8,041	8,054	8,058	8,058	8,04	8,043	8,05	8,053	8,038	8,04	8,015	8,060	8,058	8,005	8,012	7,991	8,007	8,010	8,012
X_{Mg}	0,14	0,11	0,10	0,13	0,15	0,10	0,12	0,10	0,09	0,11	0,10	0,12	0,19	0,18	0,17	0,16	0,17	0,16	0,17	0,17	0,17	0,11	0,11	0,13	0,12	0,08	0,13	0,08	0,1
X_{alm}	0,56	0,39	0,37	0,48	0,58	0,84	0,81	0,73	0,69	0,76	0,77	0,82	0,60	0,51	0,52	0,49	0,52	0,49	0,5	0,47	0,53	0,54	0,57	0,72	0,71	0,80	0,77	0,79	0,77
X_{sps}	0,27	0,45	0,52	0,32	0,25	0,04	0,06	0,14	0,20	0,12	0,11	0,02	0,20	0,19	0,2	0,19	0,20	0,20	0,22	0,23	0,19	0,31	0,26	0,08	0,11	0,08	0,06	0,09	0,09
X_{prp}	0,09	0,04	0,04	0,07	0,10	0,09	0,11	0,08	0,06	0,09	0,09	0,11	0,14	0,11	0,11	0,09	0,10	0,09	0,10	0,1	0,11	0,06	0,07	0,11	0,10	0,07	0,11	0,07	0,08
X_{grs}	0,08	0,12	0,07	0,14	0,08	0,03	0,02	0,04	0,04	0,04	0,03	0,05	0,06	0,18	0,17	0,22	0,18	0,21	0,18	0,21	0,17	0,10	0,10	0,09	0,08	0,05	0,06	0,05	0,06

X_{MG}= Mg/(Fe+Mg)* Total Fe as FeO+Fe_2O_3

also occur as matrix phases. Apatite is most abundant in the Mn-rich core region (also outlined by the low-Ca annulus) and is rare in the outer parts of the garnet except very close to the rim, where a few large grains are located (Figure 5, below). Monazite increases in abundance from garnet core to rim to matrix, but is entirely lacking from the low-Ca zone. Xenotime occurs only as a matrix phase.

PCM-516 Garnet. Pelitic schist from the garnet-staurolite-zone, which contains a mineral assemblage of quartz + plagioclase + K-feldspar + muscovite + biotite + garnet. Garnet porphyroblasts are subhedral, 0.3-2.5 mm in diameter, pseudopentagonal and poiquiloblastic (Figure 2d). They contain inclusion trails of quartz and platy ilmenite that preserve evidence of an earlier fabric occurring at a high angle to the main fabric, which corresponds to a crenulation cleavage. An inclusion-free rim separates the core from the external fabric. Garnet is associated with symmetrical and asymmetrical pressure shadows. The fabric outside of garnet porphyroblasts generally displays evidence of recrystallization and grain-size

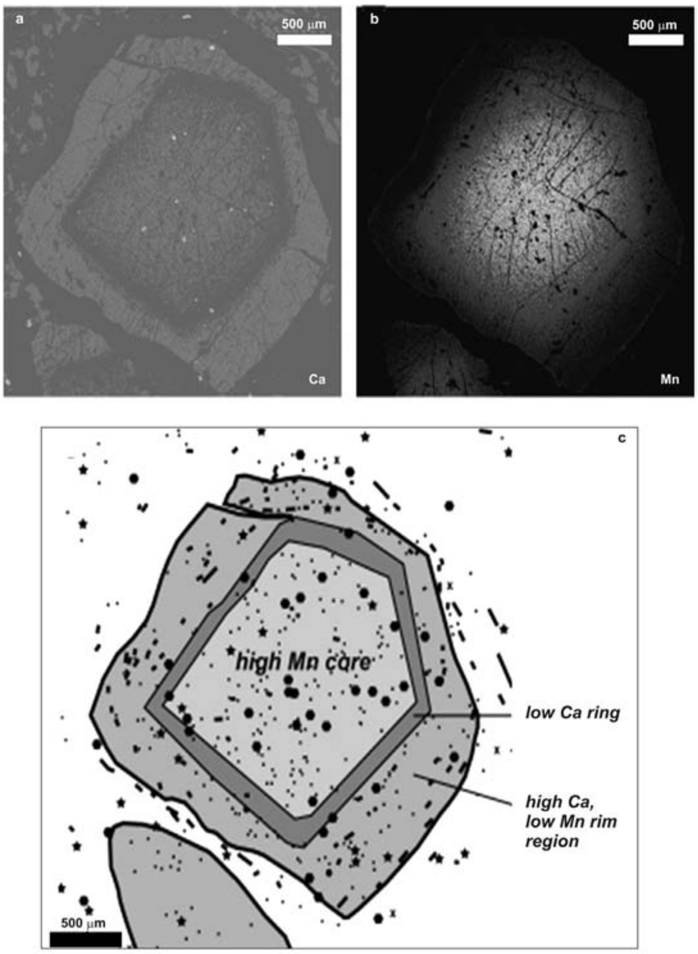

Figure 5. Above, X-ray compositional maps in garnet from sample PCM-361 (garnet-staurolite zone). (a) Occurrence of a low-Ca annulus characterized by sharp pentagonal and straight outlines. (b) Relationship between the euhedral zone of high-Mn region and the low-Ca annulus. In the X-ray maps, the elemental distributions are indicated by white color for the highest and black color for the lowest concentration. (c) Sketch of same garnet showing that the low-Ca annulus lacks of inclusions. Accessory mineral phases are indicated by black dots (apatite), x marks (xenotime), stars (monazite) and dashes (ilmenite). Courtesy of Donna Whitney.

coarsening, respect to the inclusions within garnet. A second stage of garnet growth is indicated by the inclusion-free rim that separates the core from the discordant external fabric. Garnet shows decreasing Mn from the core (34 mol%) to the rim (16 mol%). Fe and Mg increase from core to rim, with a small decrease in Fe/Fe+Mg. This garnet is characterized by a small reversal in zoning near the rim. Fe, Mg and Mn distributions are strongly correlated with each other, whereas Ca distribution is not (Figures 3d, 6b). Ca decreases outwards and reaches a minimum at mid-region (4 mole %), then increases towards the rim. Inclusions in garnet are ilmenite and quartz in the core region. Irregular patches of calcite occur within garnet and in the matrix and may be texturally late, but we note that the distribution of calcite in garnet is confined within the core region, which is bordered by the low-Ca ring. Calcite does not occur in the grossular-rich outer core/rim of the garnet, although the outer core/rim region is highly fractured. Trace elements were not analyzed.

PCM-514 Garnet. Calc-silicate rock from the garnet-staurolite-zone characterized by a mineral assemblage of quartz + plagioclase + K-feldspar + garnet + calcic amphibole. A very interesting texture is observed in this sample, with clusters of numerous fine- to medium-grained crystals of garnet, which are 0.1-3.3 mm in diameter, anhedral to subhedral and pseudohexagonal and rounded shape, containing abundant quartz inclusions throughout its core (Figure 2f). Other inclusions are epidote, plagioclase, biotite and ilmenite. Each crystal of garnet has major element zoning (Figure 3c), but no detectable trace element zoning in the analyzed elements. The grossular component displays a complex oscillatory zoning, fluctuating between 17 and 24 mol%, opposite to the trend in zoning in almandine (Figure 6c). From core to rim, spessartine decreases and Fe/(Fe+Mg) increases. Analyzed garnets have at least two high-Ca annuli. The variable grossular content may be related to reactions involving other calcic phases in this rock calcic amphibole, plagioclase, epidote). The garnet core, defined as the region within the low-Ca ring, contains abundant mineral inclusions. Quartz is most common, but epidote, plagioclase, K-feldspar, calcic amphibole, biotite, magnetite and ilmenite also occur. Patchy calcite is present in the garnet and appears to be related to fractures. Calcite occurs both within and beyond the low-grossular ring in the outer core. Figure 8a shows that Na is antipathetic with Ca, which suggest that the anorthite content in plagioclase varies with the grossular content in garnet and therefore it is necessary a source of Ca in addition to the garnet and plagioclase. On the other hand, Ti show a positive correlation with Ca (Figure 8b), which could reflect the consumption of a Ti-rich mineral phase such as ilmenite or rutile during garnet growth. Similar oscillatory zoning has been reported by other authors (e.g., Jamtveit *et al.*, 1995; Holten *et al.*, 1997; Ivanova *et al.*, 1998; Jamtveit, 1999; Pollok *et al.* 2001), probablye due to fluctuations in supersaturation, which might have originated from external (boiling, fluid mixing, temperature, and pressure fluctuations) or internal factors, resulting from self-organization in the interplay of fluid convection and crystal growth in the near vicinity of the growing crystals (Jamtveit *et al.* 1995; Holten *et al.* 1997; Pollok *et al.* 2001).

PCM-420 Garnet. Quartz-feldespatic pelitic rock from the garnet-staurolite-zone that contains a mineral assemblage of quartz + plagioclase + K-feldspar + biotite + garnet. Garnet occurs as large (1-2 mm in diameter) subhedral and subrounded porphyroblasts with cores densely packed with very fine inclusions of quartz and minor ilmenite with no preferred orientation that give the host crystal a spongy appearance and inclusion-free rims or as small (0.5-1 mm in diameter) subhedral and subrounded grains with inclusion-free cores (Figure 2b). The fabric outside of garnet porphyroblasts shows recrystallization and grain-size coarsening, respect to the inclusions within garnet. Small crystals of magnetite occurs adjacent to garnet. Garnet exhibits growth zoning: from core to near rim, there is an increase in Mg (from 3 to 12 mol%) and a decrease in Mn (from 43 to 6 mol%; Figure 6d) and in Ca (from 18 to 8 mol%), with a small decrease in the Fe/(Fe+Mg) ratio. Concentrations of Mn, Mg and Fe in the cores of the small garnets correspond with near-rim compositions in the larger crystals, but Ca composition is not similarly systematic. The concentration of Ca in the cores of small garnets does not correspond to near-rim compositions in the larger crystals. No discontinuity in the compositional zoning of Mn occurs at the boundary between the inclusion-rich core and the inclusion-free rim. Within the high-Mn region, which also corresponds to an inclusion-rich region in the garnet, zoning is not concentric about the core (Figure 6d).

PCM-473 Garnet. Pelitic schist from the staurolite-kyanite-zone. It is characterized a mineral assemblage of quartz + plagioclase + muscovite + biotite + garnet + staurolite. Garnet in this sample oc-

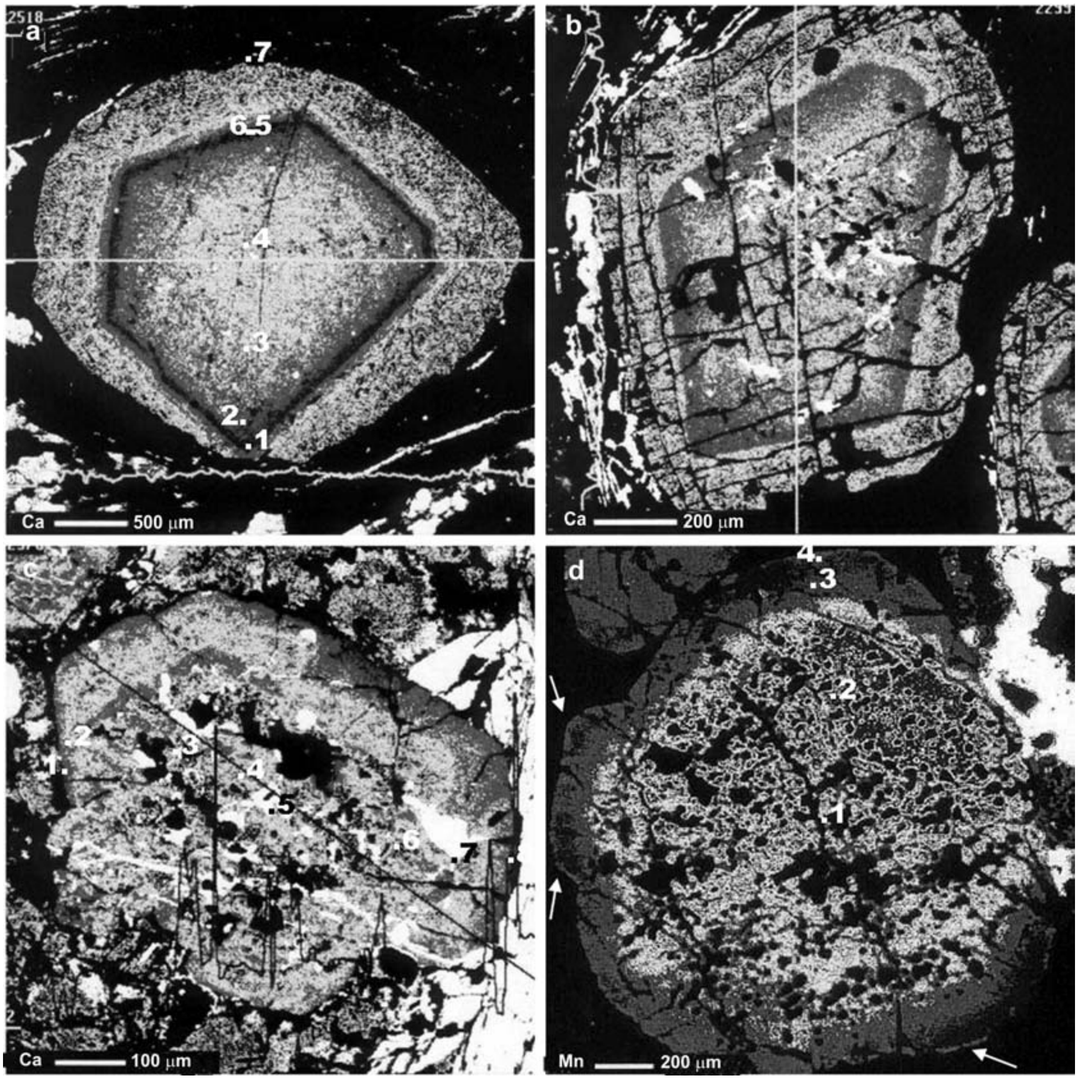

Figure 6. X-ray compositional maps in pelitic garnets from the garnet-staurolite zone. (a) and (b) illustrate low-Ca annuli with sharp pentagonal outlines in garnet from samples PCM-361 and PCM-516, respectively. In (a), at the bottom of the garnet, the low-Ca annulus is truncated against biotite; white areas correspond to calcite (garnet core region and matrix) and Ca-rich plagioclase (matrix). (c) Cyclic Ca zoning in garnet from sample PCM-514 with low- and high-Ca annuli with sharp hexagonal outlines. (d) Mn distribution in garnet from sample PCM-420, showing a small reversal zoning at rim. Numbered spots are keyed to analyses in Table 2. In the X-ray maps, the elemental distributions are indicated by white color for the highest and black color for the lowest concentration.

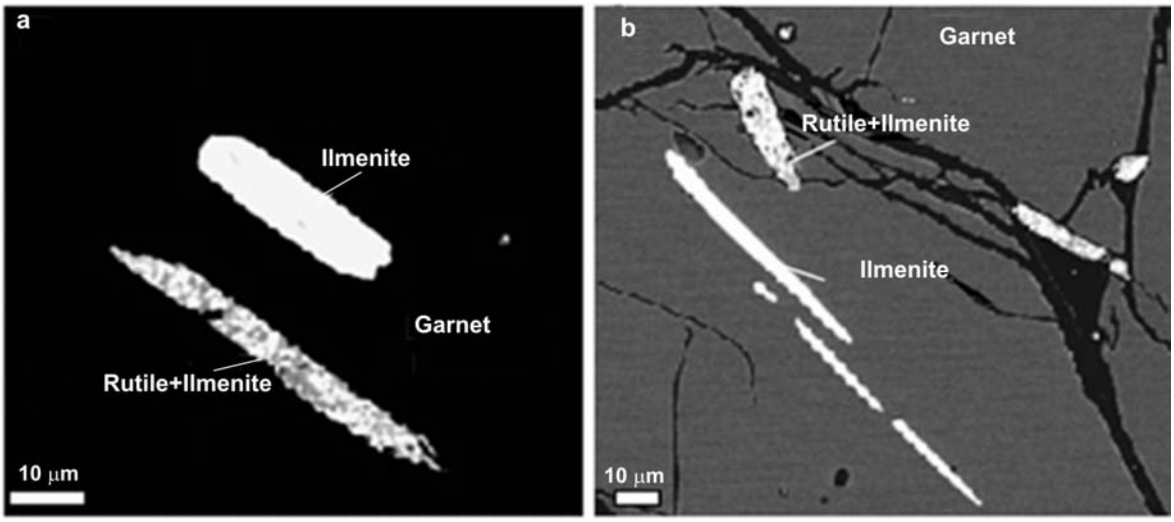

Figure 7. Back-scattered electron images of garnet in sample PCM-361 (garnet-staurolite zone), which contains ilmenite inclusions. (a)-(b) Unreacted crystal of ilmenite and adjacent pseudomorph of rutile after ilmenite.

curs as large porphyroblasts, which are up to 5 mm in diameter, anhedral (generally elongated) and contain a small number of inclusions of quartz, biotite, muscovite, plagioclase, ilmenite and magnetite. It has been highly cracked and partially replaced by quartz, muscovite and sillimanite (Figure 2e). Fibrolite commonly occurs within muscovite that is associated to garnet or as minute crystals sometimes penetrating quartz grains, which develop embayment in garnet, within which the polymorph of Al_2SiO_5 also occurs. The staurolite usually occurs as relicts in muscovite. Rutile occurs only as a matrix phase. Garnet exhibits reverse zoning, with a decrease in Mg (from 11 to 6 mol%), Figure 9a, and increase in Mn (from 7 to 10 mol%), Figure 9b, from core to rim and a small increase in the Fe/(Fe+Mg) ratio. Composition is more homogenous in the interior of the crystal and Ca content increases slightly within the outer core (5-7 mol%), where it reaches a maximum, then decreases to 5 mol% at rim, developing a low-Ca annulus (Figure 9c).

Reaction history

A detailed discussion of the reaction history among major mineral phases in metapelitic rocks of the Silgará Formation at the southwestern Santander Massif has been presented by Ríos (1999) and Ríos *et al.* (2003). Therefore, only metamorphic reactions in garnet-bearing pelites will be considered here. The typical Barrovian progression of metamorphic reactions in these rocks involve low-grade garnet growth, intermediate-grade garnet consumption during staurolite producing and high-grade resumption of garnet growth during kyanite producing at expenses of staurolite, which is similar to what reported Kohn & Malloy (2004).

The first appearance of garnet was the result of a Fe-Mg-Mn continuous reaction. The characteristic garnet of the garnet zone is almandine-rich and probably grew by two continuous reactions:

(1) Chl + Ms = Grt + Bt + Qtz + H_2O

(2) Chl + Ms + Qtz = Grt + Bt + H_2O

which can explain the formation of almandine and pyrope in garnet, but the high Ca amount observed in the garnet core or rim suggests that a Ca-rich phase also participated in the garnet-forming reaction. The source of Mn is inferred to be Mn-rich epidote, probably enclosed in clinozoisite or other matrix minerals. The garnet isograd reaction is

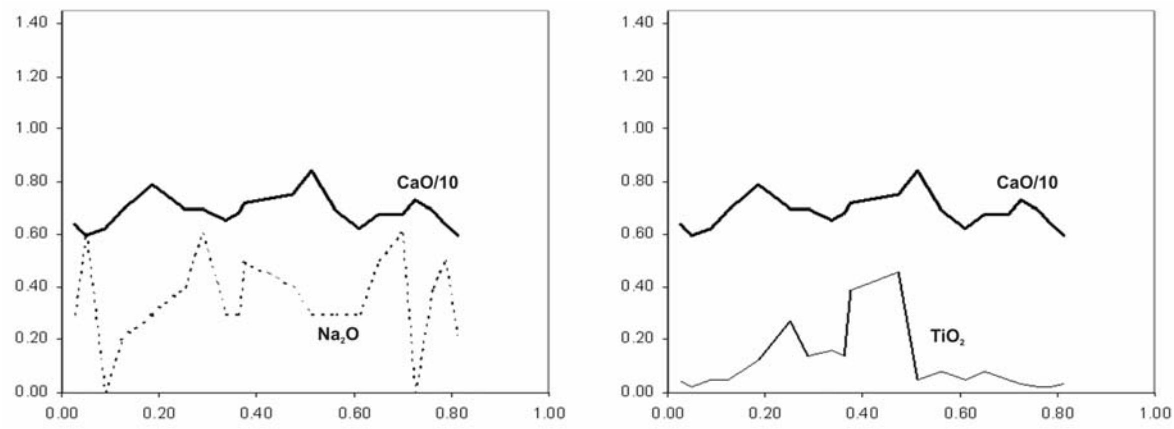

Figure 8. Zoning profiles rim-core-rim in garnet from sample PCM-514 (garnet-staurolite zone), showing the correlation between the weight percent of CaO and the (a) Na_2O and (b) TiO_2 contents. Lower axis indicates distance (mm). Left axis indicates concentration (wt%).

strongly dependent on bulk rock composition and specially the MnO and CaO contents. In rocks of high amount of those components, garnet may appear at temperatures below 450°C whereas in rocks of low amount of them, garnet may not appear to well above 500°C (Spear, 1993). Respect to the cyclic zoning observed in calc-silicate rocks (e.g., sample PCM-514, Figure 6c), we consider that the high- and low-Ca annuli in garnet may have grown, respectively, by the following reactions

(3) Chl + Ms + Ep = Grt + Bt + Pl + Ca-Amp + + Bt + H_2O,

(4) Chl + Pl + Ms + Qtz = Grt + Bt + Ca-Amp + + H_2O

However, the behavior of Ca-rich fluids should be evaluated further by considering the trace element concentrations in garnet. According to Pollok *et al.* (2001), oscillatory zoning in garnet can be explained through two different sets of processes: local growth dynamics vs external forcing mechanisms.

At the staurolite isograd, the first appearance of staurolite can be related to two reactions. Textural evidence shows that staurolite may be produced at the expense of garnet by the discontinuous reaction

(5) Grt + Chl + Ms = St + Bt + Qtz + H_2O

In garnet-free assemblages, staurolite may be produced by the continuous reaction

(6) Chl + Ms = St + Bt + Qtz + H_2O

which can be deduced from metamorphic textures, considering that staurolite grew mainly in phyllosilicate-rich layers (Graebner and Schenk, 1999). When chlorite is completely consumed, as staurolite becomes less abundant it may be preserved as inclusions or armoured relics in muscovite and garnet growth can be explained by the reaction

(7) St + Bt + Qtz = Grt + Ms + H_2O

Staurolite may dissapears with further growth of garnet at the kyanite isograd as a result of the discontinuous reaction

(8) St + Ms + Qtz = Ky + Grt + Bt + H_2O

If garnet is not involved, the staurolite breakdown is produced by the continuous reaction

(9) St + Ms + Qtz = Al_2SiO_5 + Bt + H_2O

which reflects lower temperatures than the discontinuous reaction (6) and P-T conditions nearly independient of the MnO and CaO contents of the rock. However, if garnet breaks down as sillimanite

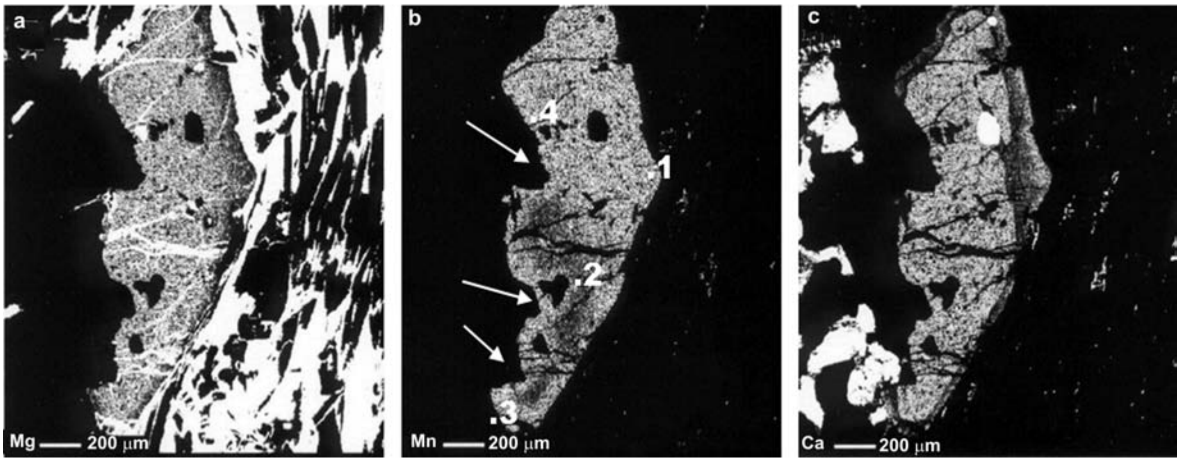

Figure 9. X-ray compositional maps showing (a) Mg, (b) Mn and (c) Ca distribution in garnet from sample PCM-473 (staurolite-kyanite zone). White arrows indicate embayments. Numbered spots are keyed to analyses in Table 2. In the X-ray maps, the elemental distributions are indicated by white color for the highest and black color for the lowest concentration.

is produced, so the initial growth of sillimanite may be considered to result from two separate continuous reactions operating simultaneously

$$(10)\ St + Ms + Qtz = Sil + Bt + H_2O$$

$$(11)\ Grt + Ms = Bt + Sil + Qtz$$

Chemical zoning and sillimanite inclusions in muscovite and quartz may indicate decrease in pressure after the formation of sillimanite by reaction (9) and during staurolite-consuming reactions (increasing temperature).

There is textural evidence to support the first appearance of kyanite in pelitic rocks of the Silgará Formation by the polymorphic reaction andalusite $\rightarrow$ kyanite. On the other hand, a net reaction such as andalusite $\rightarrow$ sillimanite must not have occurred at some point during metamorphism, because we don't really know if the andalusite reacted directly to produce the sillimanite or if the andalusite was first dissolved in a fluid phase, with the fluid phase carrying the dissolved components to a new location where the fluid then precipitated the sillimanite. However, the presence of sillimanite, kyanite and andalusite in the area or in some samples seems to suggest a more complex P-T metamorphic evolution.

Discussion

In this study we reveal a number of important observations regarding the major and trace element zoning and its correlation with accesory mineral phases in garnet-bearing pelites and associated lithologies of the Silgará Formation at the southwestern Santander Massif. Fe, Mg and Mn zoning is strongly correlated with respect to the degree of local equilibrium in contrast with Ca zoning that does not mimic zoning of those elements exactly (e.g., Chernoff & Carlson, 1997; Spear & Daniel, 1998). This strong correlation supports the hypothesis that these elements achieved a close approach to local equilibrium during garnet growth. If variations of these elements were produced only by local variations in bulk composition, then mass balance and phase equilibrium considerations would predict antithetic zoning of Fe, Mg and X_{Fe} with respect to Mn. The chemical zoning in the analyzed garnets may be originated by growth zoning, as a result of changing external conditions (pressure, temperature or bulk rock chemistry) and by diffusion zoning also due to changing external conditions, but with no growth or consumption of garnet. According to Spear (1993), a change in chemical zoning character from growth zoning to diffusion zoning by progressive homogenization is attributed to diffusion with increasing metamorphic grade. However, a local metasomatic event has also played a very important role in controlling metamorphic reactions.

Major element zoning. The analyzed garnets usually show a normal zoning with Mn content decreasing from core to rim, suggesting a prograde metamorphism. A high Mn content correlates with a high Fe/(Fe+Mg), which suggests that areas of high Mn content formed at lower temperature. Therefore, Mn zoning can be used as a time line in these rocks (Spear and Daniel, 1998). Crystal size distribution (CSD) analysis of garnets is consistent with continuous nucleation and growth of garnet throughout the garnet crystallization episode (Ríos *et al.*, 2003), which indicates that large garnets nucleated early and the smallest garnets nucleated last. In contrast to the observations of Chernoff & Carlson (1997) for garnets in the Picuris Range, New Mexico, high-Mn, low-Mg+Fe cores or low-Mn, high-Mg+Fe cores do not correlate with garnet size in the Silgará Formation. However, the strong correlation of Mn and Fe, regardless of garnet crystal size and spatial distribution, suggests a homogenous distribution of these divalent cations in the intergranular medium during garnet growth. Ca zoning can exhibit different trends than the Fe-Mn-Mg and is generally unrelated to zoning patterns in Fe, Mn and Mg, although in some cases Ca and Mn zoning patterns are spatially related (e.g., sample PCM-361, Figure 5a, 5b). It is well known that changes in the reactant mineral phases and product assemblages occur at different times during the reaction history of garnet crystals of different size and, therefore, they can not be the result of any event affecting the entire rock, such as a change in pressure, temperature or fluid composition but they reflect kinetic factors that cause Ca to fail achieving chemical equilibrium during garnet growth. Although garnet outlines are sometimes slightly rounded (e.g., PCM361, Figure 6a; PCM-516, Figure 6b), it is possible to observe that their rims were basically parallel to the euhedral low-Ca annuli and that the majority of garnet consumption occurred at the corners or intersections of growth crystal faces of garnet. A likely explanation for the difference in appearance of the annuli is that a particular thin section plane did not necessarily pass through the centre of the garnet and in some cases a high-annuli at core could be missed. Garnet shows abrupt variations in Ca distribution from core to rim, probably due to the consumption of Ca-enriched mineral phases in garnet-producing reactions, developing zoning patterns with euhedral low-Ca annuli (Figures 6a, 6b) parallel to the garnet outlines, which is typical of growth zoning and suggest that very little diffusion took place after growth (Chernoff & Carlson, 1999). Cal-silicate rocks contain a variety of Ca-rich phases (e.g., epidote, plagioclase, Ca amphibole and apatite) in addition to garnet. If the consumption or production of these phases and the changes in how Ca and other elements are locally partitioned between garnet and other minerals, accounts for garnet zoning, there should be trends in zoning in other Ca-rich phases. Matrix plagioclase typically displays normal zoning, with an increase in X_{An} spatially associated with a decrease in X_{grs} of garnet rims (Ríos *et al.*, 2003). Low-Ca annuli within garnets are unlikely to have been caused by resorption of garnet because the bands are euhedral. A garnet resorption would be expected to produce an irregular, embayed garnet margin and an overgrowth on such irregular boundary should produce a subhedral to anhedral annulus, which has not been observed in this study. A sharp decrease of grossular content from core to the mid-region has been interpreted by Menard & Spear (1993) as produced by resorption of garnet during productions of staurolite or loss of epidote from the assemblage, which is unlikely because the garnet core is euhedral. A change in mineral assemblage may account for some of the zoning trends observed, but to explain the complex oscillatory zoning observed in calc-silicate rocks (sample PCM-514, Figure 6c), this would require appearance and disappearance of Ca-rich phases or some other process that control fluctuations in the availability of elements. The Ca-rich bands in garnet may correlate with the breakdown of epidote as well as with the presence of a Ca-rich fluid. Garnet growth continued with decreasing grossular content after each of these events, showing that Ca was fractionated into garnet, plagioclase and/or calcic amphibole. Ti and Ca contents in garnet from sample PCM-514 are positively correlated, which may reflect consumption of ilmenite or rutile to liberate Ti during growth of Ca- rich garnet or metasomatic addition of Ti. There is not doubt that a complex oscillatory zoning as described here has a controversial origin and we agree with Stowell *et al.* (1996) in the sense that it is difficult to explain it by a cyclic addition and loss of mineral phase(s) from the chemical system. Instead, it could reflect episodic metasomatism by influx of Ca-rich fluids during garnet growth near of adjacent to hydrothermal veins of quartz-epidote. Therefore, the results obtained by Ríos & Takasu (1999) for Ca concentrations would not be interpreted as event markers or as recording complex barometric histories, when in fact they reflect only local effects that can not have occurred simultaneously throughout the rock.

Trace element zoning. Analysis of the trace element zoning in garnet was done as a useful supplement to major-element zoning to improve the petrological interpretation. According to Pyle & Spear (1999), trace elements zoning in garnet growing in a close system depends on the presence or absence of “saturing” mineral phases such as xenotime for Y, xenotime, apatite or monazite for P and ilmenite, titanite or rutile for Ti. However, the accessory phases that likely reflect interactions with major phases could be xenotime and monazite, as a consequence of reaction coupling with garnet and the high compatibility of Y in all three phases. In our case, we have documented the presence of these accessory mineral phases, but unfortunately they did not show trace element zoning, except in sample PCM-441 (Figure 4b), where Y zoning shows a remarkably euhedral core that is not really parallel to crystal faces of garnet, representing a growth zone that probably was not modified by diffusion. High-Y annuli in garnet have been reported by Pyle & Spear (1999) in staurolite-bearing samples, which may form by garnet overgrowth of proximal matrix enrichment in Y due to garnet consumption during discontinuous staurolite-forming reactions. Therefore, the high-Y annulus observed in the garnet studied from the garnet zone can not be explained by a resorption-regrowth process, which also will produce a chemical zoning characterized by an asymmetric annulus with steeper slopes and embayed and irregular shapes. However, the growth history of this garnet can be represented by a period of garnet growth at an approximately constant activity of Y (xenotime stable), followed by garnet at much lower Y activity (xenotime absent). Lanzirotti (1995) describes different mechanisms for annular rings of high-Y in garnet, such as open system-fluid infiltration, garnet resorption and renewed growth (unlikely argument for Y zoning described above), changes in garnet growth rates and comsumption of Y-enriched mineral phases. Therefore, the production of an annulus without garnet resorption requieres that the accessory-phase-out reaction be essentially discontinuous or the result would be a gradual, rather than abrupt, increase in garnet major or trace element content (Pyle & Spear, 1999). Hickmott & Spear (1992) concluded that concentrations of Y, Zr and REE in garnet should vary with Ca concentrations because these elements susbtitute into epidote-group minerals. Therefore, reactions involving consumption of these phases should supply both Ca and these trace elements for garnet growth. Unfortunately, garnet from sample PCM-514 does not show trace-element zoning in Y and therefore is difficult to correlate it with Ca in garnet. The addition of calcium would control chemical reactions producing garnet (X_{grs} increases), plagioclase (X_{An} increases), calcic amphibole and epidote, whereas reactions in absence of metaso- matism would return X_{grs} and X_{An} to previous levels. Xenotime is present only as a matrix accessory phase in sample PCM-361 (Figure 5c), which can be interpreted as a stable mineral phase throughout the entire growth history of garnet. At this respect, Pyle & Spear (1999) consider that the scarcity of matrix xenotime at grades above the garnet-zone in garnet-bearing pelites implies that the growth of garnet is accompanied by the consumption of xenotime. Monazite is a common accessory mineral in samples from the higher metamorphic zones (garnet-staurolite and staurolite-kyanite), being virtually absent at garnet-grade. Monazite inclusions occur in garnet (e.g., PCM-361, Figure 5c), suggesting that they grew before or during growing of garnet. Garnet growth should be previous to or synchronous with matrix monazite growth. Its growth may be related to the prograde consumption of allanite as been reported in different studies, assuming P is derived from apatite (e.g., Catlos *et al.*, 2001). Although it is probable that a precursor LREE mineral was present, garnet, plagioclase and phyllosilicates host sufficient P and LREEs and the reaction between them could stabilize monazite (Kohn & Malloy, 2004). Where analyses are not disrupted by the presence of inclusions, Ti concentration decreases from core to rim. The increasing concentration towards the rim in garnet may be a result of changes in the Ti-bearing minor phase assemblage from ilmenite-rutile in the garnet core to rutile in the garnet rim. Accesory ilmenite, titanite and rutile coexist with the silicates. Inclusions of ilmenite (by far the most prominent Ti-bearing phase) in garnet have been partly replaced by rutile as observed in Figure 7 and show from core to rim an increase in MnO and a decrease in FeO. Apatite is abundant in all rocks throughout the garnet outboard and in the matrix. Accessory phases such as zircon, monazite, titanite, epidote and allanite may contain significant Y, but these should be of limited modal extent in the samples examined with respect to garnet to explain why there is not apparent trace element zoning in garnet (except for Y in sample PCM-441).

Diffusion and resorption. Garnet usually shows a normal zoning with Mn content decreasing from core to rim, although a minimum Mn content near rim (e.g., sample PCM-420, Figure 6d) sometimes is observed, and this type of zoning is characterized as reversal zoning, which in many cases reflects post-peak resorption and reequilibration during cooling by elemental diffusion during retrograde metamorphism. Whitney and Ghent (1993) consider that no significant increase in Mn at garnet rims suggests no major late metamorphic resorption of garnet. However, a resorption process cannot explain a reversal zoning in euhedral garnet. Possible explanations involve growth or post-crystallization modification. In the case of the former, asymmetric zoning can be explained by overgrowth of Mn-rich phase(s) (top half of crystal in Figure 6d) as well as a lower Mn phase by garnet at low temperature (so that diffusion was limited and Mn was confined to the vicinity of the overgrown phase(s); e.g., Hirsch *et al.*, 2003). The core, represented by a low Mn concentration, is not situated in the geometrical center of the grain, implying either asymmetrical growth or that a significant amount of resorption has taken place, which is compatible with the corroded appearance of the rim. Mn is not concentric about individual parts of the garnet, but rather is zoned in irregular, amoeba-like shapes, a pattern that reflects fast growth along grain boundary surfaces and slower dissolution and replacement of quartz inclusions (Spear & Daniel, 1999). However, we consider that this garnet where is in contact with progressive shear zones displays a tectonic dissolution, as revealed by the chemical zoning, which is abruptly truncated against the main metamorphic foliation of the rock. Chemical zoning in garnet from sample PCM-473 can be affected by a post-growth thermal history. Garnet zoning is reversal in this sample and is best explained by diffusion during partial resorption of first stage garnet, with a second stage of growth near the outer rim of garnet, marking the onset of a new prograde garnet producing reaction. Resorption is compatible with the corroded appearance of the rim and also with the traditional interpretation of the low-Mg (Figure 9a) and high-Mn (Figure 9b) rim. Figure 9c illustrates partial preservation of a low-Ca annulus at the outermost rim, which is truncated by dissolution and resorption of garnet, developing embayments At rim, the chemical zoning are patchy and the Mn or Mg (samples PCM-361, PCM-420, PCM-514 or PCM-516) and Y (sample PCM-441) distributions are characterized by a small reversal zoning, indicating some garnet resorption and back diffusion after maximum temperature was achieved as a consequence of reaction zones of chlorite or biotite around garnet that could contain inclusions of accessory mineral phases such as xenotime, monazite, epidote, zircon or titanite that can incorporate significant amounts of Y as proposed in differet studies (e.g., Wopenka *et al.*, 1996; Heinrich *et al.*, 1997; Finger *et al.*, 1998).

Conclusions

We propose that our zoning and textural observations are most consistent with a continuous garnet growth process, involving various Ca-rich phases, and that garnet growth may have varied in terms of different garnet producing reactions during prograde metamorphism. The occurrence of inclusion-rich and inclusion-free zones in garnet has been explained by a change in the rate of garnet growth (Yang and Rivers, 2001), i.e., garnet growth in the inclusion-rich zones must have been sufficiently rapid to allow entrapment of abundant inclusions. Therefore, we can interpret inclusion-poor rims and inclusion-rich cores as representing different growth rates, which is supported here by the occurrence of garnet showing low-Ca annuli lack of inclusions (e.g., PCM-361 and PCM-516) and high-Mn inclusion-rich core (e.g., PCM-420). In sample PCM-361, for example, the high Ca / low Mn rim zone contains apatite, monazite and ilmenite aligned parallel to the margins of the garnet, whereas the euhedral low-Ca annulus within the garnet corresponds to a change in mineral inclusion abundance, but does not correspond to a change in the mineral inclusion assemblage itself (Figures 5, 6a). The low- and/or high-Ca annuli may be used as time markers during garnet growth history and truncation of annuli is not only an evidence of tectonic dissolution in progressive shear zones as proposed by Ríos *et al.* (2003) but also an excellent indication of subsequent garnet resorption. Accessory-phase assemblages may consider an early garnet growth at the expense of chlorite or biotite, with resultant xenotime consumption and production of monazite. Most importantly, this study shows that monazite crystallization is not an isolated event, but occurs throughout the metamorphic history of the rock. We have shown that valuable petrogenetic information can be obtained from major and trace-element distribution in pelitic and associated rocks of the Silgará Formation and that a complete understanding of reaction history may be achieved if accessory phases are considered. However, our interpretation could be tested by running Gibbs method simulations, utilising internally consistent thermodynamic datasets and relevant activity-composition models.

Acknowledgements

This research forms part of the M.Sc. program carried out by C. Ríos at Shimane University. We are very grateful to the Instituto Colombiano para el Desarrollo de la Ciencia y la Tecnología “Francisco José de Caldas” (COLCIENCIAS), as well as the Universidad Industrial de Santander, entities that through Grant No. 1102-05-083-95 financially supported fieldwork (Research Project: “Metamorphism and associated metallogeny of the Santander Massif, Eastern Cordillera, Colombian Andes”). We are indebted to the Research Center for Coastal Lagoon Environments at Shimane University for allowing us the use of the electron microprobe analyzer for acquisition and assistance of major element data. We also thank Dr. D. Whitney from the Department of Geological and Geophysics at University of Minnesota for her assistance with the adquisition of major and trace element data, substantial contributions and help in manuscript preparation.

References

Anderson, D.E., and Buckley, G.R (1973). Zoning in garnets: Diffusion models. Contributions to Mineralogy and Petrology, Vol. 40, pp. 87-104.

Boinet, T., Bourgois, J., Bellon, H., et Toussaint, J. (1985). Age et repartition du magmatism premesozoique des Andes de Colombie. Comptes rendus hebdomadaires des séaces de L’Académie des Sciences. Serie D: Sciences Naturalles, Vol. 300, pp. 445-450.

Bucher, K., and Frey, M. (1994). Petrogenesis of Metamorphic Rocks. 6th edition Complete revision of Winkler’s textbook. Springer-Verlag, Berlin Heidelberg, Germany.

Carlson, W.D. (1989). The significance of intergranular diffusion to the mechanisms and kinetics of porphyroblast crystallization. Contributions to Mineralogy and Petrology, Vol. 103, pp. 1-24.

Catlos, E., Harrison, T., Kohn, M., Grove, M., Lovera, O., Ryerson, F., and Upreti, B. (2001). Geochronologic and thermobarometric constraints on the evolution of the Main Central Thrust, central Nepal Himalaya. Journal of Geophysics Research, Vol. 106, pp. 16177–16203.

Chamberlain, C.P., and Conrad, M.E. (1993). Oxygen-isotope zoning in garnet: A record of volatile transport. Geochimica et Cosmochimica Acta, Vol. 57, pp. 2613-2629.

Chernoff, C., and Carlson, W. (1997). Disequilibrium for Ca during growth of pelitic garnet. Journal of Metamorphic Geology, Vol. 15, pp. 421-438.

Chernoff, C. and Carlson, W. (1999). Trace element zoning as a record of chemical disequilibrium during garnet growth. Geology, Vol. 27, pp. 555-558.

Cygan, R.T., and Lasaga, A. (1982). Crystal growth and the formation of chemical zoning in garnets. Contributions to Mineralogy and Petrology, Vol. 79, pp. 187-200.

Dörr, W., Grösser, J., Rodríguez, G., and Kramm, U. (1995). Zircon U-Pb age of the Paramo Rico tonalite-granodiorite, Santander Massif (Cordillera Oriental, Colombia) and its geotectonic significance. Journal of South American Earth Sciences, Vol. 8, pp. 187-194.

Erambert, M., and Austrheim, H. (1993). The effect of fluid and deformation on zoning and inclusion patterns in poly-metamorphic garnets. Contributions to Mineralogy and Petrology, Vol. 115, pp. 204-214.

Finger, F., Broska, I., Roberts, M.P., and Schermaier, A. (1998). Replacement of primary monazite by apatite-allanite-epidote coronas in an amphibolite facies granite gneiss from the eastern Alps. American Mineralogist, Vol. 83, pp. 259-272.

Gibson, H., Carr, S., Brown, R., and Hamilton, M. (2004). Correlations between chemical and age domains in monazite and metamorphic reactions involving major pelitic phases: an integration of ID-TIMS and SHRIMP geochronology with Y-Th-U X-ray mapping. Chemical Geology, Vol. 211, pp. 237-260.

Goldsmith, R., Marvin, R., and Mehnert, H. (1971). Radiometric ages in the Santander Massif, Eastern Cordillera, Colombian Andes. U.S. Geological Survey Professional Paper, Vol. 750, pp. 41-49.

Heinrich, W., Andrehs, G., and Franz, G. (1997). Monazite-xenotime miscibility gap thermometry. I. An empirical calibration. Journal of Metamorphic Geology, Vol. 15, pp. 3-16.

Hickmott, D., and Shimizu, N. (1990). Trace element zoning in garnet from the Kwoiek area, British Columbia: disequilibrium partitioning during garnet growth? Contributions to Mineralogy and Petrology, Vol. 104, pp. 619-630.

Hickmott, D., and Spear, F. (1992). Major- and trace-element zoning in garnets from calcareous pelites in the NW Shelburne Falls Quadrangle, Massachusetts: Garnet growth histories in retrograded rocks. Journal of Petrology, Vol. 33, pp. 965-1005.

Hickmott, D.D., Shimizu, N., Spear, F.S., and Selverstone, J. (1987). Trace-element zoning in a metamorphic garnet. Geology, Vol. 15(6), pp. 573-576.

Hirsch, D., Prior, D., and Carlson, W. (2003). An overgrowth model to explain multiple, dispersed high-Mn regions in the cores of garnet porphyroblasts. American Mineralogist, Vol. 88, pp. 131-141.

Hollister, L.S. (1966). Gamet zoning: An interpretation based on the Rayleigh fractionation model. Science, Vol. 154, pp. 1647-1651.

Holten, T., Jamtveit, B., Meakin, P., Cortini, M., Blundy, J., and Austrheim, H. (1997). Statistical characteristics and origin of oscillatory zoning in crystals. American Mineralogist, Vol. 82, pp. 596–606.

Ivanova, T.I., Shtukenberg, A.G., Punin, Y.O., Frank-Kamenetskaya, O.V., and Sokolov, P.B. (1998). On the complex zonality in grandite garnets and implications. Mineralogical Magazine, Vol. 62, pp. 857–868.

Jamtveit, B., Wogelius, R.A., and Fraser, D.G. (1993). Zonation patterns of skarn garnets: Records of hydrothermal system evolution. Geology, Vol. 21, pp. 113-116.

Jamtveit, B., and Hervig, R.L. (1994). Constraints on transport and kinetics in hydrothermal systems from zoned garnet crystals. Science, Vol. 263, pp. 505-508.

Jamtveit, B., Ragnarsdottir, K.V., and Wood, B.J. (1995). On the origin of zoned grossular-andradite garnets in hydrothermal systems. European Journal of Mineralogy, Vol. 7, pp. 1399–1410.

Jamtveit, B. (1999). Crystal growth and intracrystalline zonation patterns in hydrothermal environments. In Growth, Dissolution and Pattern Formation in Geosystems, B. Jamtveit and P. Meakin Eds, p.65–84, Kluwer Academic Publishers, Dordrecht, The Netherlands.

Kohn, M., and Malloy, M. (2004). Formation of monazite via prograde metamorphic reactions among common silicates: Implications for age determinations. Geochimica et Cosmochimica Acta, Vol. 68, pp. 101–113.

Kretz, R. (1983). Symbols for rock-forming minerals. American Mineralogist, Vol. 68, pp. 277-279.

Lanzirotti, A. (1995). Yttrium zoning in metamorphic garnets. Geochimica et Cosmochimica Acta, Vol. 59, pp. 4105-4110.

Lasaga, A. (1983). Geospeedometry: An extension of geothermometry. In S.K. Saxena, Ed., Kinetics and equilibrium in mineral reactions, Springer-Verlag, New York. p. 81-114.

Menard, T., and Spear, F. (1993). Metamorphism of calcic pelitic schists, Strafford Dome, Vermont: Compositional zoning and reaction history. Journal of Petrology, Vol. 34, pp. 977-1005.

Ordoñez, J. (2003). Petrology and geochemistry of the granitoids at the Santander Massif, Eastern Cordillera, Colombian Andes. Unpublished Master Thesis, Shimane University, Matsue (Japan), 150p.

Pollok, K., Jamtveit, B., and Putnis, A. (2001). Analytical transmission electron microscopy of oscillatory zoned grandite garnets. Contributions to Mineralogy and Petrology, Vol. 141, pp. 358–366.

Pyle, J. and Spear, F. (1999). Yttrium zoning in garnet: Coupling of major and accessory phases during metamorphic reactions. Geological Materials Research, Vol. 1, pp. 1-49.

Ríos, C. (1999). Chemical compositions of the constituent minerals and P-T conditions of the low-grade Silgará Formation metamorphic rocks in the Santander Massif, Eastern Cordillera, Colombian Andes. Unpublished Master Thesis, Shimane University, Matsue (Japan), 207p.

Ríos, C., y García, C. (2001). Primera ocurrencia de los tres polimorfos de Al_2SiO_5 en las rocas metapelíticas de la Formación Silgará, región suroccidental del Macizo de Santander, Cordillera Oriental, Andes Colombianos. Boletín de Geología UIS, Vol. 23, pp. 51-59.

Ríos, C., García, C., andyle, J., & Takasu, A. (2003). Tectono-metamorphic evolution of the Silgará Formation metamorphic rocks in the southwestern Santander Massif, Colombian Andes. Journal of South American Earth Sciences, Vol. 16, pp. 133-154.

Ríos, C., and Takasu, A. (1999). Chemical zoning of garnet from the low-grade metamorphic rocks of the Silgará Formation, Santander Massif, Eastern Cordillera (Colombian Andes). Geosciences Reports of Shimane University, Vol. 18, pp. 97-107.

Schwandt, C., Papike, J., and Shearer, C. (1996). Trace element zoning in pelitic garnet of the Black Hills, South Dakota. American Mineralogist, Vol. 81, pp. 1195-1207.

Skelton, A., Annersten, H., and Valley, J. (2002). δO^{18} and yttrium zoning in garnet: time markers for fluid flow? Journal of Metamorphic Geology, Vol. 20, pp. 457-466.

Spear, F. (1993). Metamorphic Phase Equilibria and Pressure-Temperature-Time Paths. Mineralogical Society of America, Washington, DC.

Spear, F., and Daniel, C. (1998). Three-dimensional imaging of garnet porphyroblast sizes and chemical zoning: Nucleation and growth history in the garnet zone. Geological Materials Research, Vol. 1, pp. 1-42.

Stowell, H., Menard, T., and Ridgway, Ch. (1996). Ca-metasomatism and chemical zoning of garnet in contact-metamorphic aureoles, Juneau Gold Belt, southeastern Alaska. The Canadian Mineralogist, Vol. 34, pp. 1195-1209.

Tracy, R.J., Robinson, P., and Thompson, A.B. (1976). Garnet composition and zoning in the determination of temperature and pressure of metamorphism: Central Massachusetts. American Mineralogist, Vol. 61, pp. 762-775.

Ward, D., Goldsmith, R., Cruz, B., Jaramillo, C., y Res- trepo, H. (1973). Geología de los Cuadrángulos H-12, Bucaramanga y H-13, Pamplona, Departa- mento de Santander. U.S. Geological Survey e Ingeominas. Boletín Geológico, Vol. XXI, 132p.

Whitney, D., and Ghent, E. (1993). Prograde reactions and garnet zoning reversals in staurolite schist. British Columbia: significance for thermobarometric interpretations. Journal of Metamorphic Geology, Vol. 11, pp. 779-788.

Wopenka, B., Jolliff, B.L., Zinner, E., and Kremser, D.T. (1996). Trace element zoning and incipient metamictization in a lunar zircon: application of three microprobe techniques. American Mineralogist, Vol. 81, pp. 902-912.

Yang, P., and Rivers, T. (2001). Chromium and manganese zoning in pelitic garnets and kyanite: spiral, overprint and oscillatory (?) zoning patterns and the role of growth rates. Journal of Metamorphic Geology, Vol. 19, pp. 455-474.

Yang, P., and Rivers, T. (2002). The origin of Mn and Y annuli in garnet and the thermal dependence of P in garnet and Y in apatite in calc-pelite and pelite, Gagnon terrane, western Labrador. Geological Materials Research, Vol. 4 (http://gmr.minsocam/Papers/v4/v4n1).

Young, E.D., and Rumble, D., III (1993) The origin of correlated variations in in-situ $^{18}0/^{16}0$ and elemental concentrations in metamorphic garnet from southeastern Vermont, USA. Geochimica et Cosmochimica Acta, Vol. 57, pp. 2585-2597.